Chapter 2 Literature Review

2.1 Anodic Aluminum Oxide (AAO)

Nanoporous anodic aluminum oxide (AAO) formed by anodization has been widely studied during the last few decades. Because of their relatively regular structure with narrow size distributions of pore diameters and interpore spacings, porous alumina membranes are used for the fabrication of nanometer scale composites [1]. The pore structure is a self-ordered hexagonal array of cells with cylindrical pores of variable sizes with diameters of 25 nm to 300nm with depths exceeding 100 mm depending on the anodizing conditions used. The geometry of anodic porous alumina may be schematically represented as a honeycomb structure which is characterized by a close-packed array of columnar hexagonal cells[2], each containing a central pore normal to the substrate, as shown in Fig. 2-1 (a) [3]. However, the geometry of the anodic porous alumina usually obtained is far from the idealized model; that is, the cells are irregular polygons, and the arrangement of the cells and pores is not ideal hexagonal. This irregularity of the porous structure causes distortion of the cross section of the pores and broadening of the pore diameter distribution. These properties make anodized aluminum a desirable material for many microfabricated fluidic devices, quantum-dot arrays, polarizers, magnetic memory arrays, high-aspect-ratio microelectromechanical systems, and photonic crystals. This nanoscale pattern formation phenomenon by electrochemical reactions has also attracted many theoretical studies to decipher its instability mechanism but without much success. Masuda *et al.* [4] reported self-organized pore growth, leading to a densely packed hexagonal pore structure for certain sets of parameters. But highly regular polycrystalline pore structures occur only for a quite small processing window,

whereas an amorphous pore structure can be obtained for a very wide range of parameters without substantial change in morphology. The former models based only on field distribution cannot easily explain this behavior. The self-organized arrangement of neighboring pores in hexagonal arrays can be explained by any repulsive interaction between the pores.

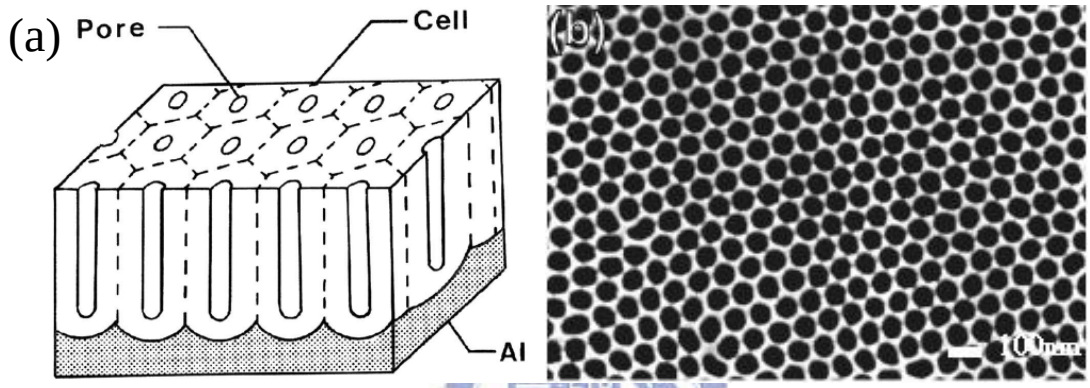

Figure 2-1 (a) Schematic drawing of the idealized structure of anodic porous alumina. (b) SEM micrographs of the bottom view of anodic alumina layers. Anodization was conducted in 0.3 M oxalic acid at 1 °C at 40 V.

The basic mechanism behind pore formation phenomenon still awaits explanation and a self-consistent theory. When aluminum is anodized in an acid solution, such as sulfuric (H_2SO_4), oxalic ($H_2C_2O_4$), and phosphoric (H_3PO_4) acids, deep nanopores can continuously grow, with diameters varying between ten and several hundred nanometer and lengths up to several microns. Both the barrier-type and pore-type AAO usually start from fairly smooth aluminum surface, but with pits formed at lattice imperfections or by electropolishing [5].

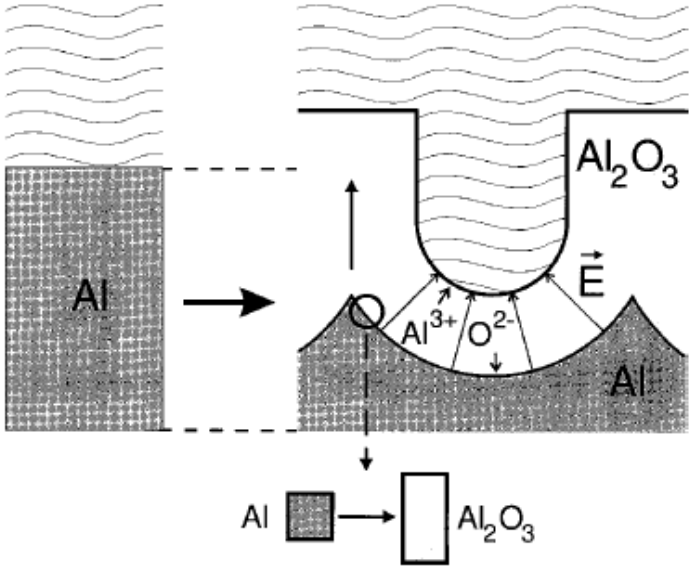

Figure 2-2 Expansion of aluminum during anodic oxidation. On the left the level of the unoxidized metal surface is depicted.

In order to explain the effect of self-organization, the situation during steady state pore growth has to be considered in Fig. 2-1 and Fig. 2-2. Pores grow perpendicular to the surface with an equilibrium of field-enhanced oxide dissolution at the oxide/ electrolyte interface and oxide growth at the metal/oxide interface [6]. While the latter is due to the migration of oxygen containing ions (O^{2-}/OH^-) from the electrolyte through the oxide layer at the pore bottom, Al^{3+} ions which simultaneously drift through the oxide layer are ejected into the solution at the oxide/electrolyte interface. The fact that Al^{3+} ions are lost to the electrolyte has been shown to be a prerequisite for porous oxide growth, whereas Al^{3+} ions which reach the oxide/electrolyte interface contribute to oxide formation in the case of barrier oxide growth [7]. The atomic density of aluminum in alumina is by a factor of two lower than in metallic aluminum. A possible origin of forces between neighboring pores is therefore the mechanical stress which is associated with the expansion during oxide formation at the metal/oxide interface. Since the oxidation takes place at the entire

pore bottom simultaneously, the material can only expand in the vertical direction, so that the existing pore walls are pushed upwards. Under usual experimental conditions the expansion of aluminum during oxidation leads to less than twice the original volume, since Al^{3+} ions are mobile in the oxide under the electric field, so partly the oxidized aluminum does not contribute to oxide formation[8]. During the steady-state growth of films under constant-potential conditions, cells with almost identical size must generate a regular arrangement of close-packed arrays of hexagonal cylinders. However, under the usual anodizing conditions, perturbations in the configuration of the grown cells result in a large number of defects in the cell arrangement. It is assumed that during anodization at a specific potential, almost perturbationless growth becomes feasible resulting in a highly ordered structure.

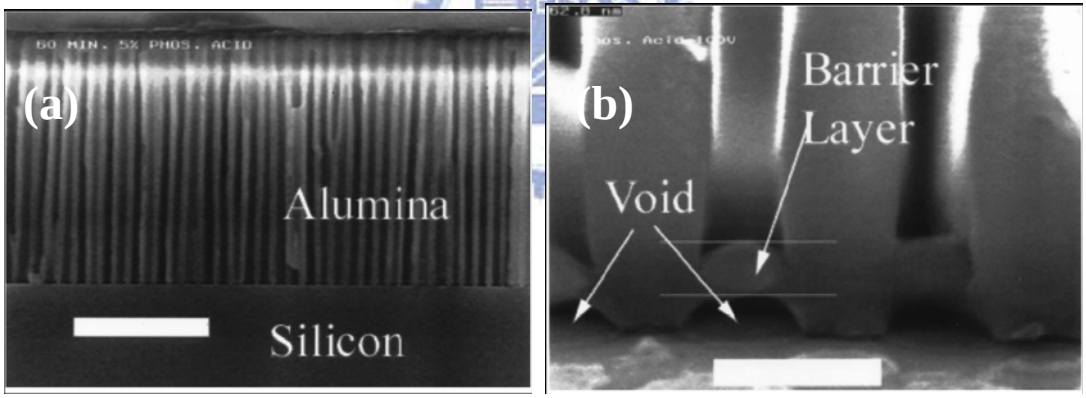

Figure 2-3 (a) Cross-sectional SEM image of 2-mm-thick porous alumina mask anodized at 60 V for 5 min followed by a 1 h pore widening etch. The white bar is 1 mm long. (b) SEM image of barrier layer features were observed on Si. The white bar is 200 nm long [9].

A practical approach of evaporated film of aluminum on silicon in Fig. 2-3 was reported [9]. The characteristics of the barrier layer are distinctly different than in the bulk aluminum case, allowing for the barrier layer to be thinned and removed quite

easily. The unique structure of the barrier layer allows for the alumina to be directly used as an etch mask for pattern transfer into the silicon substrate. When the aluminum is insulated from the substrate, the anodization can be performed by placing the electrical contact to the front side of the aluminum and then protecting it with wax. The resulting pores etched to completion down to the alumina–SiO_2 interface and were identical to the Si case where the current flowed vertically through the substrate–aluminum interface. Without the field-enhanced dissolution or the increased local temperature-enhanced dissolution, the chemical etch rate is very slow at room temperature. These coupled phenomena preferentially remove the oxide at the bottom of the pores while leaving the pore walls intact. The resulting structure is an ordered hexagonal array of cells with cylindrical pores with cell walls composed of alumina.

Furthermore, ordered pores in Fig. 2-4 by patterning the initial Al surface was reported [10-11]. The conditions for the fabrication of ideally ordered anodic porous alumina with a high aspect ratio were examined using pretextured Al in oxalic acid solution. The obtained anodic porous alumina has a defect-free array of straight parallel channels perpendicular to the surface. The channel interval could be controlled by changing the interval of the pretextured pattern and the applied voltage. However, the depth at which perfect ordering could be maintained depended on the anodizing conditions, that is, the hole array with a high aspect ratio could be obtained only under the appropriate anodizing voltage, which corresponded to that of the long-range ordering conditions in the oxalic acid solution. Under the most appropriate condition, ideally ordered channels with an aspect ratio of over 500 could be obtained. From these results, it was concluded that the long-range ordering conditions significantly influenced the growth of channels in anodic porous alumina even in/on the pretextured Al.

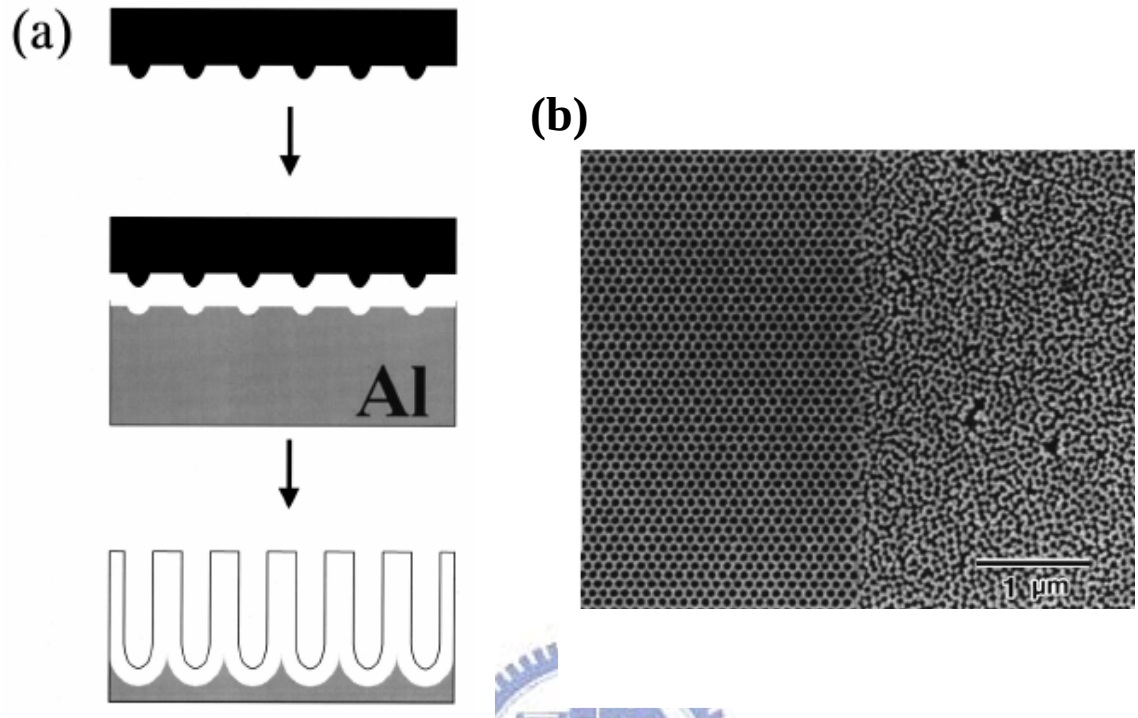

Figure 2-4 (a) Process for the fabrication of ideally ordered nanochannel array. SiC mold with hexagonally ordered array of convexes, indentation of Al with SiC mold, and anodic porous alumina. (b) SEM micrograph of surface view of ideally ordered anodic porous alumina and un-patterning anodic alumina [11].

2.2 Bottom-Up Fabrication technologies of nanodot arrays

2.2.1 Self-Assembly Copolymer / Copolymer Template

The self-assembly of two chemically different polymers covalently joined at one end into ordered nanoscale morphologies offers an attractive techniques. Recent theoretical arguments have suggested that synergistic interactions between self-organizing particles and a self-assembling matrix material can lead to hierarchically ordered structures [12-14]. The mixtures of diblock copolymers and either cadmium selenide or ferritin-based nanoparticles exhibit cooperative, coupled self-assembly on the nanoscale. In thin films, the copolymers assemble into cylindrical domains, which dictate the spatial distribution of the nanoparticles; segregation of the particles to the interfaces mediates interfacial interactions and orients the copolymer domains normal to the surface, even when one of the blocks is strongly attracted to the substrate. Organization of both the polymeric and particulate entities is thus achieved without the use of external fields, opening a simple and general route for fabrication of nanostructured materials with hierarchical order. Figure 2-5 shows fabricating ordered spatial arrangements of pre-synthesized CdS nanoparticles in thin block copolymer templates by first selectively dispersing these nanoparticles in one particular block of a diblock copolymer, in bulk, by means of dipole–dipole interactions and then using solvent selectivity to sequester CdS nanoparticles in the block copolymer thin film. A long-range, ordered morphology of CdS nanoclusters can be obtained by using patterned substrates with 400 nm shallow grooves. The incorporated nanoparticles retain the same luminescence characteristics as in the pure state [15-16].

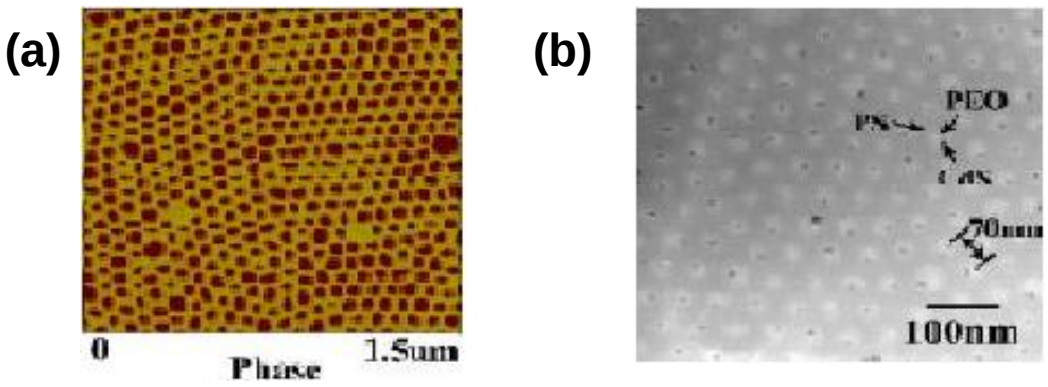

Figure 2-5 (a)AFM image of a CdS/LSEO thin film supported on a carbon-coated silicon wafer. (b) TEM image of a CdS/LSEO thin film after removal from carbon-coated silicon wafer with 1% HF solution [15].

Nanodots arrays and nanoholes in Fig. 2-6 were fabricated by evaporation onto nanoporous templates produced by the self-assembly of poly(styrene-*b*-methyl methacrylate) (P(S-*b*-MMA)) diblock copolymers. The cylindrical microdomains of the asymmetric block copolymer were oriented normal to the surface by balancing interfacial interactions of the blocks with the substrate. By selectively removing either the minor or major component, nanoporous films of PS or nanoscopic posts of PS could be produced. Thus, a template, comprising an array of hexagonally packed pores in a PS matrix or PS posts, was easily fabricated. Evaporation of metal onto the template, followed by sonication and UV degradation of the PS, left metal nanodots or a nanoporous metallic film [17-18] .

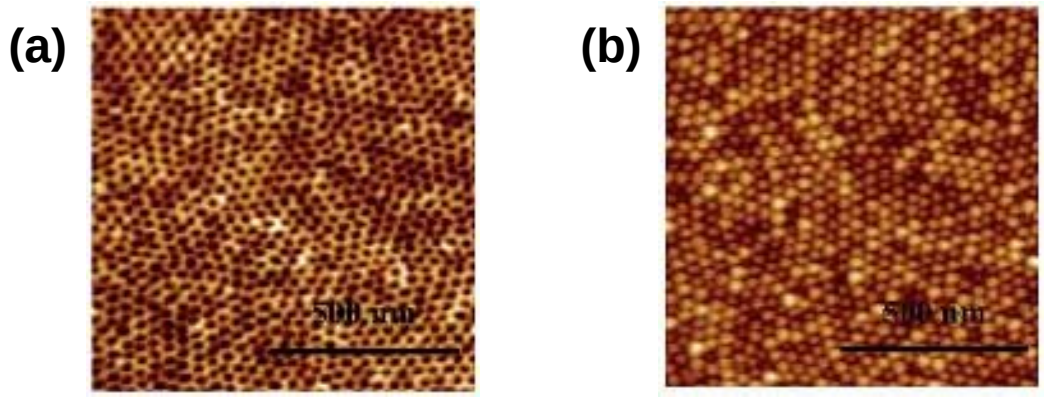

Figure 2-6 Tapping mode AFM images of (a) Block copolymer template etched by UV exposure. (b) Au/Cr dot arrays after eliminating PS matrix by the irradiation of UV [7].

2.2.2 Stranski-Krastanow Growth

One of the particularly promising approaches for fabricating large numbers of nanodots for device applications is via the spontaneous self-organization of nanoislands which occurs during Stranski-Krastanow (S-K) growth. During S-K growth, a growing epitaxial film becomes morphologically unstable as the thickness of the film exceeds a critical value (several monolayer), which results in the formation of nanoislands or nanocrystals on the substrate. The instability of a planar interface is driven by the elastic strain energy causing by the lattice mismatch or misfit between the epitaxial film and substrate. Therefore, S-K growth is constrained to a few material systems and size ranges in which the critical strain-mismatch conditions can be met (e.g. Ge\Si, InAs/GaAs, InGaAs/GaAs, InAs/InP, PbSe/PbTe, etc.) [19-22]. Figure 2-7 shows the images of strained germanium nanocrystal on prepatterned Si (001) surfaces [23]. The nanoisland arrays can then be covered with another material to create the optoelectronic devices of interest. However, manipulation of spatial arrangement and size distribution of the nanoislands remain a major problem, which is generally required for practical applications. In order to control the spatial

distribution, many efforts have been developed using variety of technique, such as selective groth on prepatterned substrate with stripe mesas [24] or on relaxed templates with dislocation networks [25]. However, it is still far from the desired control of the width of mesas or periodicity of the dislocation.

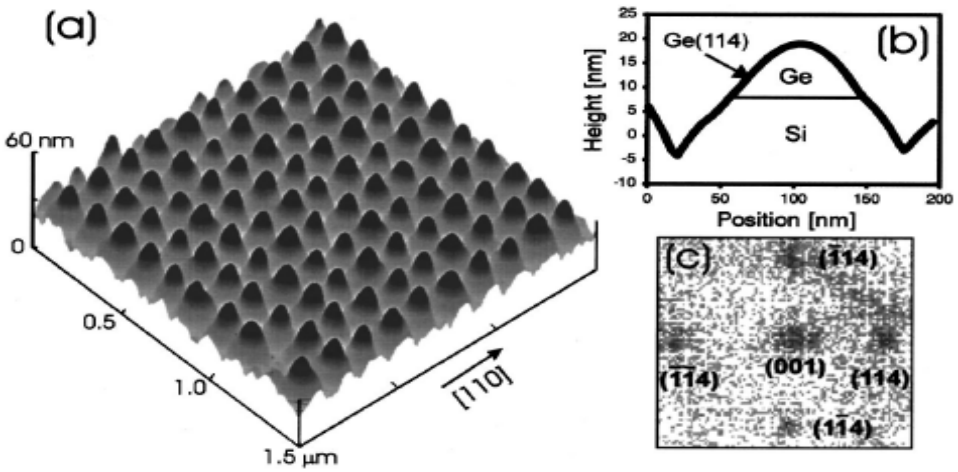

Figure 2-7 (a) AFM image of an array of Ge islands on prepatterned Si (001) surfaces. (b) Cross-sectional measurement of a typical Ge island. (c) Normal view of a histogram of the statistics of the island surface normal vectors that are measured vertically [24].

Moreover, Brune and co-workers [26] describe the fabrication of ordered, two-dimensional nanostructure arrays through nucleation of deposited metal atoms on substrates with periodic patterns defined by dislocations that form to relieve strain. The strain-relief patterns are created spontaneously when a monolayer or two of one material is deposited on a substrate with a different lattice constant [27]. Dislocations often repel adsorbed atoms diffusing over the surface, and so they can serve as templates for the confined nucleation of nanostructures from adatoms. Ordered arrays of silver and iron nanostructures on metal substrates were exhibited in Figure 2-8.

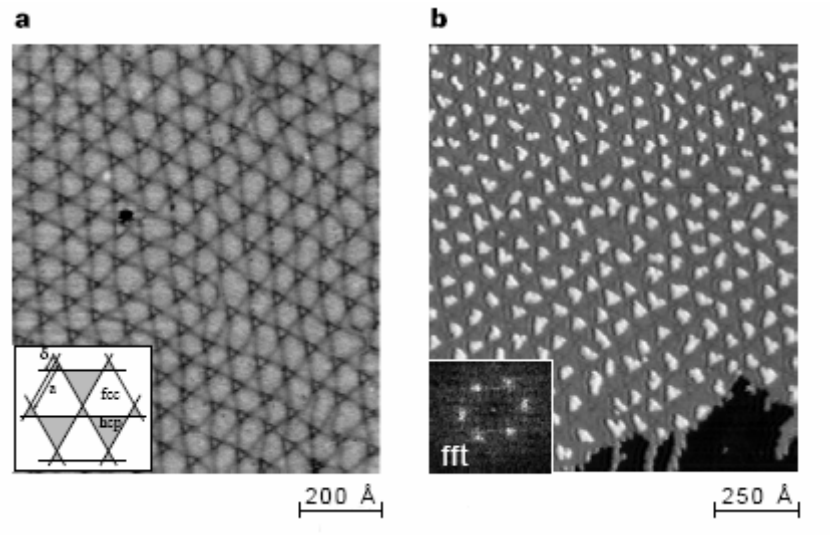

Figure 2-8 (a) STM image of the ordered dislocation network formed by the second Ag monolayer on Pt(111) and subsequent annealing to 800 K. The inset shows a model of this triangular strain relief pattern. (b) A superlattice of islands is formed on Ag deposition onto this network at 110 K. Inset, the Fourier transform of the STM image shows the high degree of order and the hexagonal symmetry of the nanostructure array. [26]

2.2.3 Chemical Colloidal Self-Assembly

Chemical self-assembly is the spontaneous orientation of a number of molecules onto an energetically favored supra-molecular structure without human intervention. Naturally occurring self-assembled systems of complex supra-molecular structures include deoxyribonucleic acid (DNA), cell membranes, chromatophores or even viruses [27-28]. The autonomous components of organic molecules modified a substrate with monolayers via self-assembly process was thus named as self-assembled monolayers (SAMs). The principal driving force for formation of these monomolecular films is specific interactions between the molecule head group and the substrate surface. Depending on the structure of the molecule, these films can resemble the organization of crystal.

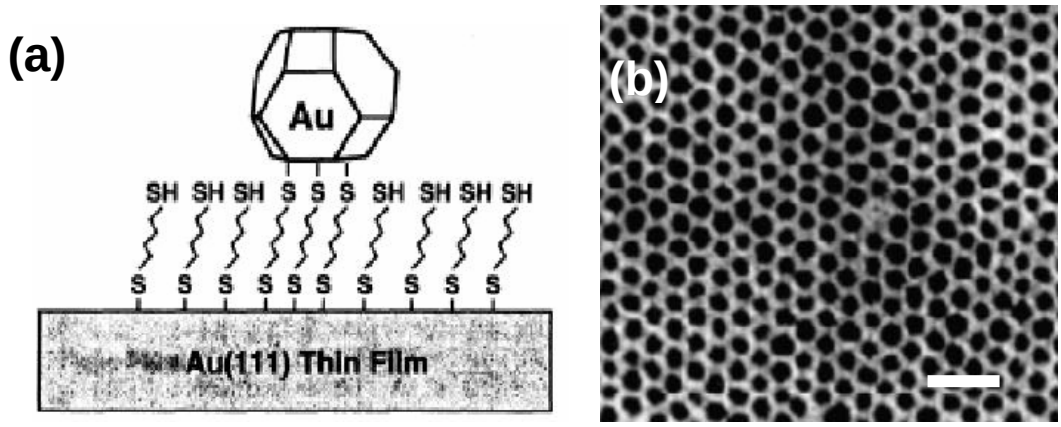

Figure 2-9 (a) schematic side-view of Au nanoparticles attached to a SAM by molecular wires [29]. (b) TEM micrographs of monolayer films of 3.7 nm Au cluster supported on thin flake of MoS_2 [30].

The SAM method in Fig. 2-9 to attach individual gold nanoparticles on the top of silicon oxide by using self-assembling molecules with functional groups on both ends [31]. Gold nanoparticles, each encapsulated by a monolayer of alkylthiol molecules, were synthesized from solution onto a substrate to form close-packed cluster monolayers. Organic interconnected displaced the alkylthiol moleculaes and covalently linked adjacent clusters in the monolayer to form a two-dimensional superlattice of metal nanodots [31]. Whetten *et* al. [32] and Fan *et* al. [33] have reported the spontaneous formation of highly ordered twoand three-dimensional superlattices from monodisperse fractions of such particles. These nanostructures can be regarded as a new class of materials whose properties can, in principle, be tuned at will by manipulating the size and spacing of their constituents. A promising route (in Fig. 2-10) to more complex nanostructures is based on the controlled covalent attachment of nanoparticles to suitably functionalized surfaces or to each other [34-37].

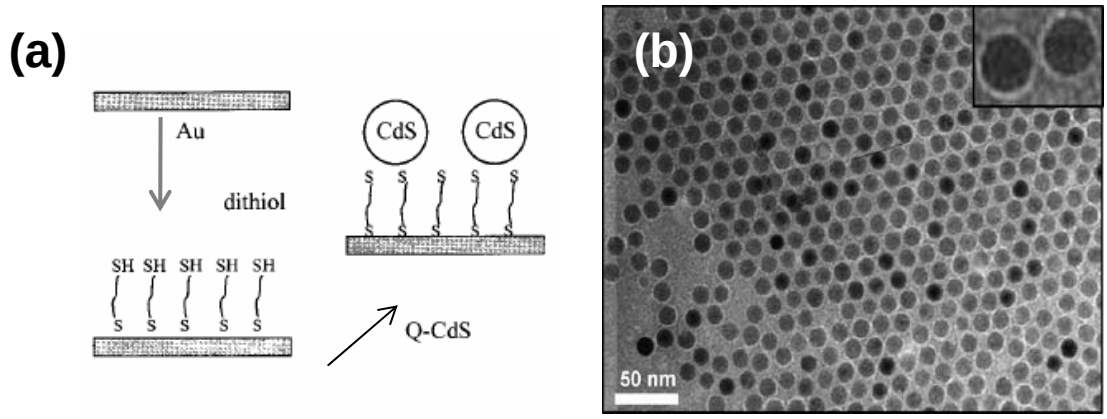

Figure 2-10 (a) Schematic representation of the layer construction of nanomaterials from Q-CdS particles and a dithiol. [35] (b) TEM micrograph of AOT-capped CdS nanoparticle array. Inset clearly shows two representative nanoparticles capped by AOT surfactant layer, with thickness of single layer ca. 14 A °[37].

2.2.4 SPM-induced Growth

Scanning probe microscope (SPM) is continuously being developed for surface modification and for the investigation of different surface properties. The ability of SPM initiate the transfer and accumulation of atoms for nanostructure fabrications is a topical aspect for further development. Nanosized islands have been grown on a sample surface by accumulating atoms from the surrounding area through directional surface diffusion initiated by the electric field of an atomic force microscope (AFM) or STM tip [38-39]. Figure 2-11 shows the STM image of germanium islands on the silicon (111) substrate created with STM at a constant tunneling current of 0.3 nA and various negative tip bias voltages [40]. As shown, the nanosized islands grew with a constant rate determined by the tip-sample bias voltage. Furthermore, SPM-induced local field oxidation is another feasible process for nanostructure fabrications. The local field oxidation process is similar to conventional electrochemical anodization except that an AFM/STM tip is used as the cathode and water from the ambient humidity is used as the electrolyte [41]. Garcia *et al.* [42] have reported the fabrication of

high-areal-density oxide dot arrays on a hydrogen-passivated silicon substrate using non-contact AFM and Cooper *et al.* [43] have reported the case of oxide array with an areal density of 1.6 Tbit/inch^2 on a titanium film using a SWCNT grown on an AFM cantilever. However, the SPM-based growth is poor efficiency for producing spatially dense nanodot arrays making it less attractive than the technique of self-organized nanodot fabrication.

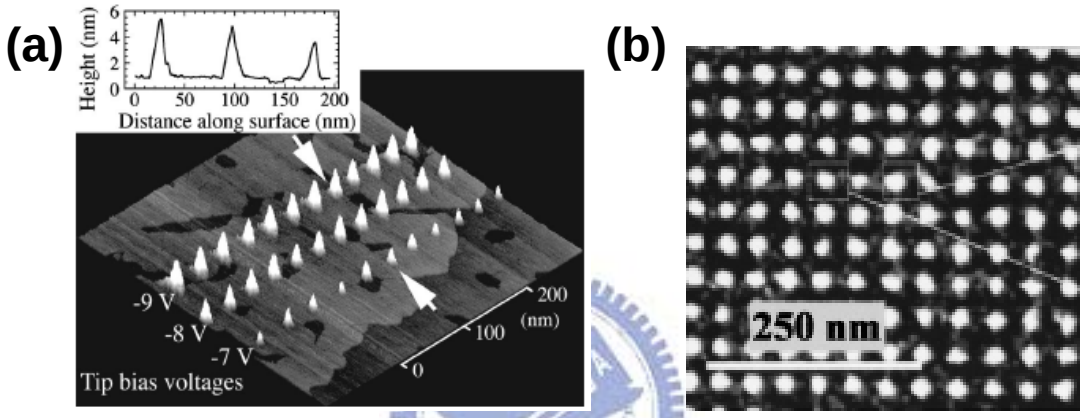

Figure 2-11 (a) STM image of germanium islands on the silicon (111) substrate covered with 2.9 bilayer of Ge at 450℃. (b) AFM image of field-induced formation silicon oxide nanodot arrays. The dots are 40 nm apart and with an average width of 10 nm. The same tip was used to grow the dots and to image them afterwards [40].

2.3 Nanodot Arrays Fabricated by AAO Template

In previous work, nanodot arrays (Fig. 2-12) on surfaces have been fabricated using an extremely thin (~300nm) freestanding anodic aluminum oxide template that served as a mask for evaporation of nanodots onto the surface [44-46]. Anodic porous alumina membranes were formed by anodizing foil Al in an acidic electrolyte. In addition to these applications, removal of the bottom part of the anodic porous alumina layer by an appropriate etching process can yield through-hole membranes. Anodic porous alumina membrane used as a mask for evaporation, and then removed the membranes. This approach has been limited to deposition of nanodots by vapor-based methods because the template is not in good contact with the underlying substrate.

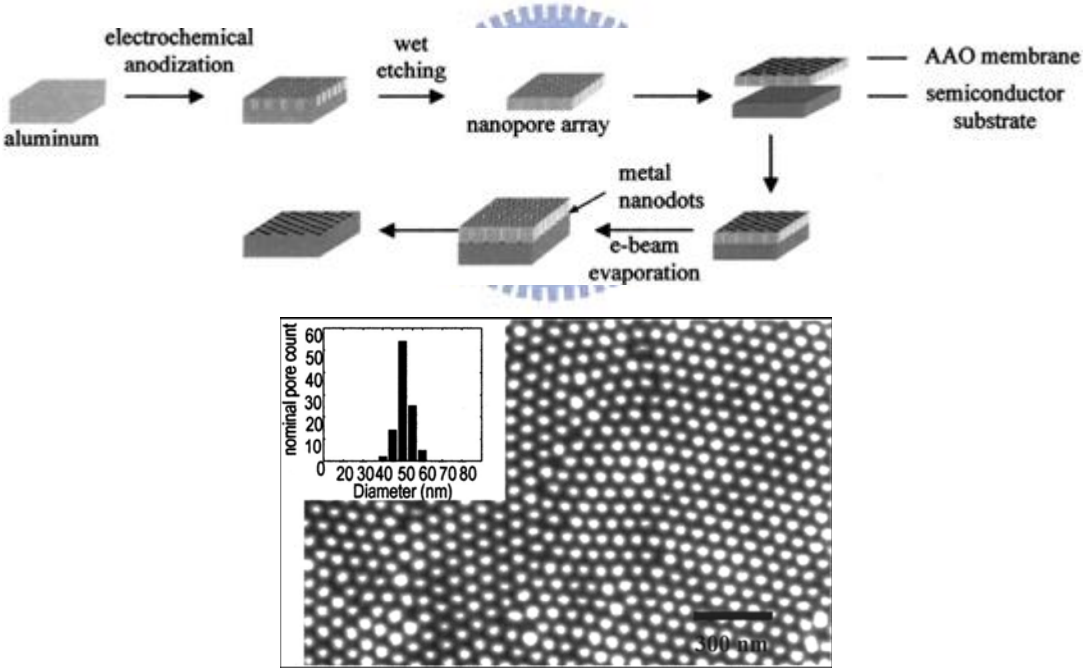

Figure 2-12 (a) schematic process used to fabricate nanodots arrays on surface using alumina template. (b) Ni nanodot arrays on Si wafer [44].

A more versatile and robust approach is to deposit an aluminum film directly on the surface and then anodize the film using the well-established condition for

aluminum foil anodization. However, during anodization an alumina barrier layer is formed at the bottom of the pores (see Figure 2-3), which prevents direct nanodots deposition onto the underlying substrate. In order to use the template to deposit nanodots onto the surface, this barrier layer must be removed. Crouse et al. [9] found that when an aluminum film is anodized on a silicon substrate, the resulting barrier layer at the pore-substrate interface is thin enough that it can be removed selectively by a short chemical etch. Without the field-enhanced dissolution or the increased local temperature-enhanced dissolution, the chemical etch rate is very slow at room temperature. These coupled phenomena preferentially remove the oxide at the bottom of the pores while leaving the pore walls intact. The obtained alumina mask had sufficient adhesion to the Si substrate. The post-etching treatment yielded through-holes in the alumina mask and could be used for the preparation of a metal nanodot array and nanohole array. Since the thickness of the barrier oxide (D_B) is proportional to the potential applied for aluminum anodization (D_B) 1.2 nm/V (applied potential), the thick barrier film formed at high voltages is a big obstacle for a subsequent electrochemical deposition. Small fluctuations in the barrier oxide thickness lead to large current fluctuations and thus very inhomogeneous filled. In this adopted thinning process, the applied potential is reduced stepwise [47]. Therefore, a well-controlled process for homogeneously thinning the barrier is vital for achieving a degree of nearly 100% filled. Because the alumina templates are fabricated directly on the substrate and remain in good contact with it, nanodots can be deposited through the template onto the substrate using either vapor-based methods or wet chemical process. Sander et al. [48] demonstrated the versatility of this template-based approach by deposition gold nanodot arrays using evaporation and higher aspect ratio gold nanorod arrays using electrochemical deposition. The templates in Fig. 2-13 do not have hexagonally ordered pores, although it is possible to produce ordered pores by

patterning the initial Al surface. The template approach is versatile and may be employed to fabricate various nanodot array systems on a range of substrates. It may be possible to use other deposition methods to produce nanodot arrays on surfaces, including chemical vapor deposition, sol-gel techniques, or chemical polymerization. The underlying substrate may be used to promote nanodots growth for example as an electrode for eletrodeposition or as a catalyst material in chemical vapor deposition. The substrate may also serve to control the structure of the nanodots in epitaxial growth processes.

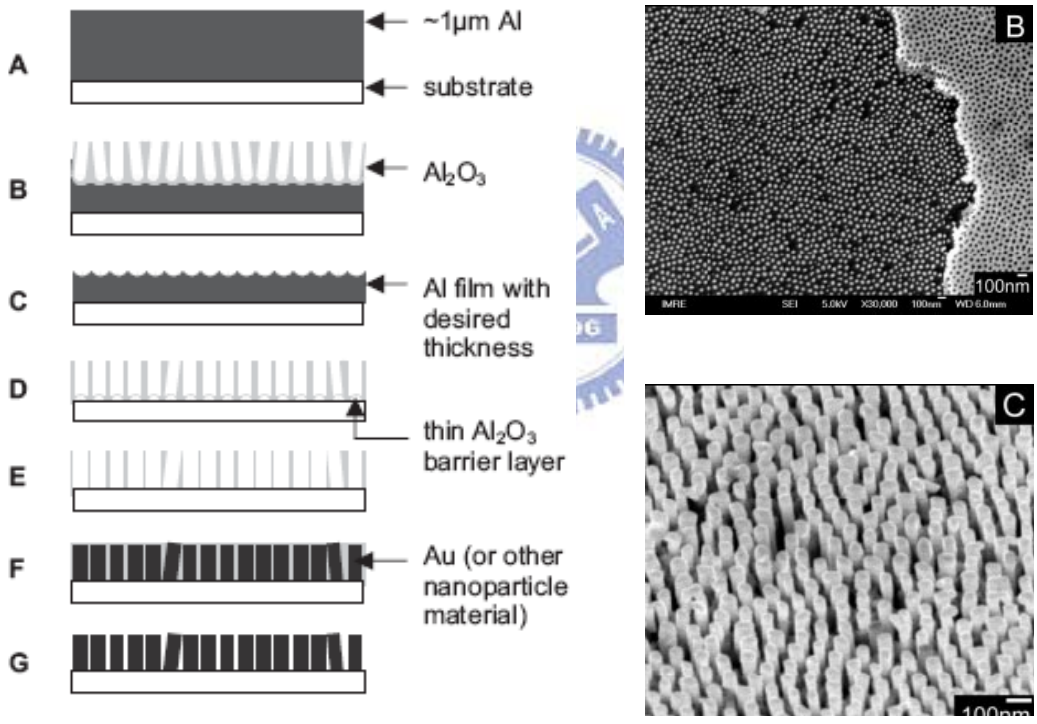

Figure 2-13 (a) schematic process used to fabricate nanodots arrays on surface using alumina template. (b) Au nanodot arrays on Si wafer. (c) Au nanorod arrays produced by electrodeposition into an alumina template on a Au/Ti/Si substrate [48]